Resonance Raman and EPR Spectroscopic Studies on Heme–Heme Oxygenase Complexes†

Jie Sun,‡ Angela Wilks,§ Paul R. Ortiz de Montellano,*,§ and Thomas M. Loehr*,‡

Department of Chemistry, Biochemistry, and Molecular Biology, Oregon Graduate Institute of Science and Technology, Portland, Oregon 97291-1000, and Department of Pharmaceutical Chemistry, School of Pharmacy and Liver Center, University of California, San Francisco, California 94143-0446

Received September 13, 1993; Revised Manuscript Received October 26, 1993®

ABSTRACT: The binding of ferrous and ferric hemes and manganese(II)- and manganese(III)-substituted hemes to heme oxygenase has been investigated by optical absorption, resonance Raman, and EPR spectroscopy. The results are consistent with the presence of a six-coordinate heme moiety ligated to an essential histidine ligand and a water molecule. The latter ionizes with a $pK_a \approx 8.0$ to give a mixture of high-spin and low-spin six-coordinate hydroxo adducts. Addition of excess cyanide converts the heme to a hexacoordinate low-spin species. The resonance Raman spectrum of the ferrous heme–heme oxygenase complex and that of the Mn(II)protoporphyrin–heme oxygenase complex shows bands at 216 and 212 cm^{-1}, respectively, that are assigned to the metal–histidine stretching mode. The EPR spectrum of the oxidized heme–heme oxygenase complex has a strongly axial signal with $g_{\parallel} \approx 6$ and $g_{\perp} \approx 2$. ^{14}NO and ^{15}NO adducts of ferrous heme–heme oxygenase exhibit EPR hyperfine splittings of ~20 and ~25 Gauss, respectively. In addition, both nitrosyl complexes show additional superhyperfine splittings of ~7 Gauss from spin–spin interaction with the proximal histidine nitrogen. The heme environment in the heme–heme oxygenase enzyme–substrate complex has spectroscopic properties similar to those of the heme in myoglobin. Hence, there is neither a strongly electron-donating fifth (proximal) ligand nor an electron-withdrawing network on the distal side of the heme moiety comparable to that for cytochromes P-450 and peroxidases. This observation has profound implications about the nature of the oxygen-activating process in the heme → biliverdin reaction that are discussed in this paper.

Heme oxygenase catalyzes the NADPH–cytochrome P-450 reductase dependent degradation of heme to biliverdin at the expense of three oxygen molecules (Tenhunen et al., 1969). Recently, heme oxygenase in the brain has been implicated in the role of CO as a neural messenger (Verma et al., 1993; Zhuo et al., 1993; Stevens & Wang, 1993). Heme oxygenase has been purified from several sources, including rat liver (Yoshida & Kikuchi, 1979), pig spleen (Yoshida & Kikuchi, 1978), bovine spleen (Yoshinaga et al., 1982), and chicken liver (Bonkovsky et al., 1990). Two isozymes, HO-1 and HO-2, have been identified (Shibahara et al., 1985; Yoshida et al., 1988; Evans et al., 1991; Maines et al., 1986; Maines, 1988). The isozymes from various species show only 50% identity in amino acid sequence, but all share a number of common features (McCoubry & Maines, 1993). Among them is a conserved 24 amino acid domain that includes an essential histidine residue (McCoubry & Maines, 1993; Ishikawa et al., 1992). The carboxyl terminal portion of the enzyme shows a low frequency of amino acid conservation, but it is highly conserved in its hydropathic profile indicating the importance of the membrane-spanning region that inserts into the endoplasmic reticulum (McCoubry & Maines, 1993; Wilks & Ortiz de Montellano, 1993a). We have recently developed a high-yield expression system that produces a soluble, fully active enzyme, HO-1C$^-$, in which the last 23 C-terminus amino acids have been deleted (Wilks & Ortiz de Montellano, 1993a).

Some important intermediates in heme oxygenase catalysis have been identified (Beale, 1993; Maines, 1992). However, key issues such as how the enzyme binds heme and activates O_2 have yet to be established. There is keen interest in obtaining structural details of the heme–heme oxygenase complex, which is important for understanding the mechanism of heme oxidation by heme oxygenase.

In this paper, we elucidate the heme binding mode in the heme–heme oxygenase (HO-1C$^-$) complex as studied by resonance Raman spectroscopy. This technique has been widely used in studying the structures of hemeproteins (Spiro, 1988). In addition, we have studied the ^{14}NO and ^{15}NO adducts of heme oxygenase by EPR[1] spectroscopy to gain information on the axial ligation of the heme substrate; these studies are patterned after the those pioneered by Kon (1968, 1969) and Yonetani and co-workers (1972).

EXPERIMENTAL PROCEDURES

Heme oxygenase and heme–heme oxygenase complex were purified according to published procedures (Wilks & Ortiz de Montellano, 1993a). Samples as purified (~600 μM) were in 10 mM potassium phosphate buffer (pH 7.4). Change of pH was achieved by two cycles of dilution (~10-fold) and reconcentration (Amicon Centricon), with 20 mM MES (pH 6.0), Tris-Ac (pH 8.5), and CHES (pH 10.0), respectively. Reduction to the ferrous state was achieved by adding 20 mM sodium dithionite solution to an argon purged sample and was

† This work was supported by grants from the U.S. Public Health Service, National Institutes of Health [DK30297 and GM32488 (P.O.d.M.) and GM34468 (T.M.L.)].

* Authors to whom correspondence should be addressed.
‡ Oregon Graduate Institute of Science and Technology.
§ University of California, San Francisco.

® Abstract published in *Advance ACS Abstracts,* December 1, 1993.

[1] Abbreviations: EPR,electron paramagnetic resonance; Hb, hemoglobin; Mb, myoglobin; PP, protoporphyrin IX; 5c and 6c, five coordinate and six coordinate, respectively; HS and LS, high-spin and low-spin electronic configurations of iron, respectively.

0006-2960/93/0432-14151$04.00/0

monitored by UV–vis spectroscopy. EPR and Raman samples of the NO adducts were prepared by addition of 5 μL of a 1 M solution of freshly prepared dithionite to an argon-purged solution of 340 μM HO-1C⁻ in a quartz EPR tube sealed by a septum. To 250 μL of the reduced heme was added 10 μL of a 1 M solution of either $Na^{14}NO_2$ (Aldrich) or $Na^{15}NO_2$ (Stohler Isotope). The resulting NO adducts were frozen in liquid nitrogen prior to recording their EPR spectra. An aliquot of this sample was removed for the Raman measurement. The cyanide adducts were made by adding appropriate amounts from a 120 mM KCN stock solution in 160 mM phosphate buffer (final pH 7.4). Mn(III)PP–heme oxygenase complex was made from Mn(III)PP chloride (Porphyrin Products, Inc.) and purified by a similar procedure to that used for heme–heme oxygenase complex (Wilks & Ortiz de Montellano, 1993a). Its reduction was also achieved by addition of 20 mM sodium dithionite solution following argon purging.

UV–vis spectra were recorded on a Perkin-Elmer Lambda 9 spectrophotometer. Samples were generally measured in glass melting-point capillary tubes (Kimax, ~1.2–1.5 mm i.d.) and placed in a black Delrin sample holder and beam mask having a 1-mm wide slot. The spectrophotometer was referenced against air and zeroed with a sample of water also contained in a capillary tube (Loehr & Sanders-Loehr, 1993).

For resonance Raman experiments, Spectra-Physics 2025-11 Kr^+, Spectra-Physics 164 Ar^+, Coherent Innova 90-6 Ar^+/599-01 (rhodamine 6G dye), and Liconix He-Cd lasers were used as excitation sources. Laser power at the sample was ~20 mW for excitations at 413.1 and 441.6 nm and ~50 mW for longer wavelengths. The samples in capillary tubes were placed in a copper rod cold finger which was immersed in an ice–water bath (90° scattering geometry) or in liquid N_2 within a Dewar (150° back-scattering geometry) previously described (Loehr & Sanders-Loehr, 1993). Spectra of the scattered light were obtained by Dilor Z24 and modified Jarrell-Ash 25-300 (Keyes et al., 1979) Raman spectrophotometers with single-channel detection. Spectral resolution was typically ~5 cm^{-1}. Although the Raman data have been background subtracted, they are presented without smoothing (unless noted). UV–vis spectra were also recorded in the same tubes before and after Raman measurements to monitor sample integrity.

X-band EPR spectra were recorded on a Varian E-109 "Century-Series" spectrometer equipped with an Air Products helium cryostat. Samples were cooled to <10 K. Individual EPR spectra were collected with a Macintosh Plus computer on a program developed by Prof. John Golbeck, and from four to eight spectra were co-added for signal averaging. The EPR spectrometer was operated near 9.3 GHz at a modulation frequency of 100 kHz, a modulation amplitude of 2 Gauss, and a microwave power of 10 μW. The signal was observed to saturate very easily, even at 50 μW, leading to loss of definition of the fine structure. All the spectral data (UV–vis, Raman, and EPR) were analyzed and plotted with "LabCalc" (Galactic Industries).

RESULTS AND DISCUSSION

Ferrous Heme–Heme Oxygenase Complex. The UV–vis and resonance Raman spectra of the ferrous heme–HO-1C⁻ complex are presented in Figures 1, 2, and 3, respectively. These spectra reveal a structural similarity with myoglobin. The UV–vis absorption maxima are at 429 and 556 nm for the ferrous heme–heme oxygenase complex, as compared with 430 and 555 nm for ferrous myoglobin (Antonini & Brunori,

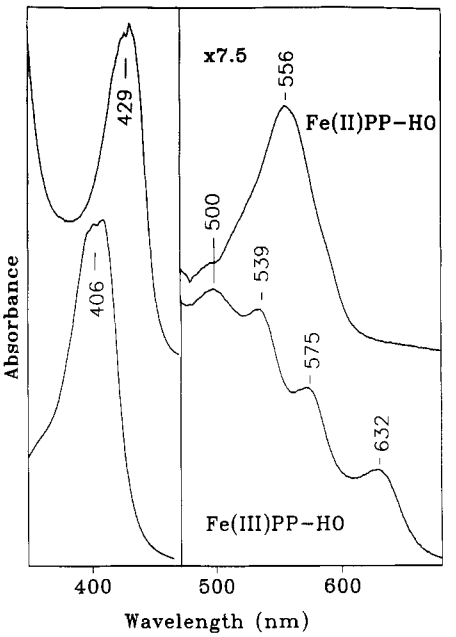

FIGURE 1: UV–vis spectra of the Fe(II)PP–HO-1C⁻ and Fe(III)-PP–HO-1C⁻ complexes (~400 μM; pH 7.4). Samples were contained in the same melting-point capillary tubes used for the Raman measurements (Figures 2 and 3). The Soret region of the latter has been smoothed (11 points).

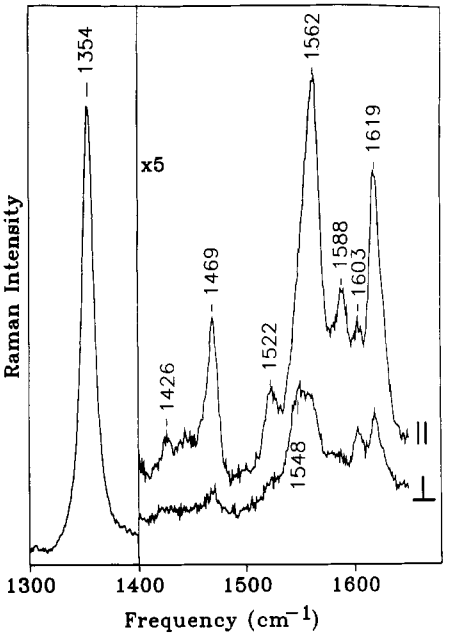

FIGURE 2: Resonance Raman spectrum of Fe(II)PP–HO-1C⁻ in the high-frequency region (441.6-nm excitation) indicating the polarization behavior >1400 cm^{-1}.

1971). The resonance Raman frequencies of porphyrin skeletal modes are also comparable with those of myoglobin or other high-spin ferrous hemoproteins having a coordinated proximal histidine ligand (Figure 2 and Table 1) (Spiro & Strekas, 1974; Rakshit & Spiro, 1974; Choi et al., 1982; Mino et al., 1988; Dasgupta et al., 1989; Palaniappan & Terner, 1989; Mylrajan et al., 1990). The presence of a proximal histidine ligand in heme oxygenase is strongly suggested by the Raman band at 216 cm^{-1} assignable to an Fe–His stretching mode (Figure 3). The low value of this frequency implies that the proximal histidine is only weakly or not hydrogen-bonded in HO-1C⁻. In myoglobin, where the proximal histidine is only weakly hydrogen-bonded, the Fe–His stretch is observed at 221 cm^{-1} (Kincaid et al., 1979; Kitagawa et al.,

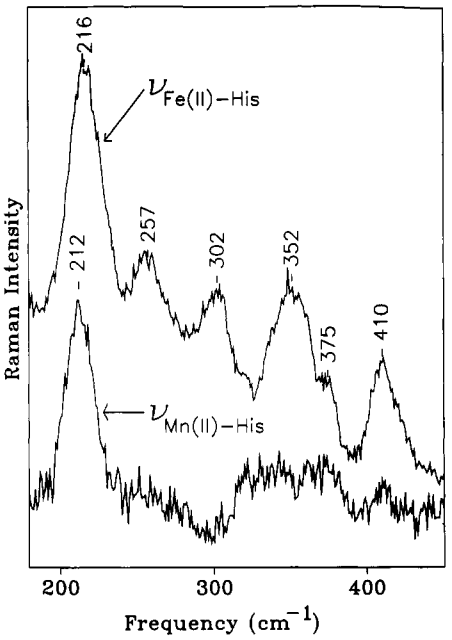

FIGURE 3: Resonance Raman spectra of Fe(II)PP–HO-1C$^-$ (upper trace) and Mn(II)PP–HO-1C$^-$ (lower trace) in the low-frequency region (441.6-nm excitation).

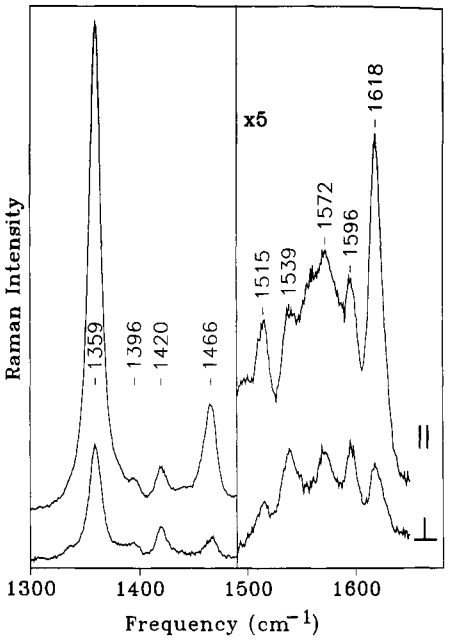

FIGURE 4: Resonance Raman spectrum of Mn(II)PP–HO-1C$^-$ in the high-frequency region (441.6-nm excitation) indicating the polarization behavior >1300 cm^{-1}.

Table 1: Porphyrin Skeletal Mode Frequencies (cm^{-1}) of High-Spin Ferrous *b* Hemes

compounds	excitation (nm)	ν_2	ν_3	ν_4	ν_{10}	ν_{11}	references
heme–HO-1C$^-$	441.6	1562	1469	1354	1603	1548	this work
Mb	?	1563	1473	1357	1607	1546	*a*
Hb	457.9	1565	1473	1358			*b*
	514.5			1358	1607	1552	
HRP	363.8	1567	1473	1359	1605	1549	*c,d*
	514.5		1472	1358	1605	1546	
CCP	514.5		1472	1358	1603		*e*
	441.6	1565	1472	1354	1603		
lignin peroxidase	413.1	1562	1478	1362			*f*
	514.5		1472	1359	1607	1554	
manganese peroxidase	413.1	1562	1473	1357			*g*
	514.5			1357	1606	1548	
(2-MeIm)FePP	457.9	1562	1471	1357			*a*
	530.8				1604	1547	

[a] Choi et al. (1982). [b] Spiro and Strekas (1974). [c] Palaniappan and Terner (1989). [d] Rakshit and Spiro (1974). [e] Dasgupta et al. (1989). [f] Mylrajan et al. (1990). [g] Mino et al. (1988).

1979; Choi & Spiro, 1983). The presence of strong hydrogen-bonding to proximal histidine increases the Fe–His stretch to ~233 cm^{-1}, while complete ionization of the proximal histidine yields an Fe–His stretch at ~246 cm^{-1} (Teraoka & Kitagawa, 1981; Smulevich et al., 1988). This observation of histidine axial ligation is consistent with site-specific mutagenesis studies, which suggest the presence of at least one essential histidine (Ishikawa et al., 1992; McCoubry & Maines, 1993). The single histidine residue located in the highly conserved 24 amino acid domain is a good candidate for this ligand (McCoubry & Maines, 1993). Mutation of this histidine to alanine abolishes heme oxygenase activity (Ishikawa et al., 1992; McCoubry & Maines, 1993). It has also been reported that treatment with diethylpyrocarbonate inactivates heme oxygenase, indicating the vital role of histidine residue(s) (Yoshinaga et al., 1982).

Mn(II)PP–Heme Oxygenase Complex. The UV–vis spectrum of Mn(II)PP–HO-1C$^-$ has three absorption peaks at 434, 559, and 594 nm (data not shown). They can be compared with those observed for Mn(II)PP–Mb (438, 560, and 598 nm), Mn(II)PP–Hb (444, 557, and 600 nm), and (2-MeIm)-Mn(II)PP (428, 556, and 588 nm), respectively (Parthasarathi & Spiro, 1987). The resonance Raman spectrum of Mn(II)PP–HO-1C$^-$ obtained with 441.6-nm excitation (Figure 4) shows polarized bands at 1359, 1466, 1572, and 1618 cm^{-1} as well as depolarized bands at 1539 and 1596 cm^{-1}. The frequencies for Mn(II)PP–Mb, Mn(II)PP–Hb, and (2-MeIm)Mn(II)PP are similar (Parthasarathi & Spiro, 1987). More importantly, we have also observed a Raman band at 212 cm^{-1} (Figure 3), which is assignable to the Mn–His stretch in the Mn(II)PP–HO-1C$^-$ complex. For Mn(II)PP–Mb and Mn(II)PP–Hb, this stretch has been observed at 215 and 216 cm^{-1}, respectively (Parthasarathi & Spiro, 1987). Above all, the resonance Raman spectrum of Mn(II)PP–HO-1C$^-$ parallels that of Fe(II)PP–HO-1C$^-$, indicating a proximal histidine axial ligation.

Ferric Heme–Heme Oxygenase Complex. Figures 5 and 6 show the UV–vis and resonance Raman spectra of ferric heme–HO-1C$^-$ complex at different pHs. These spectra indicate a profound pH influence on the heme axial coordination and spin state. At pH 6.0, the UV–vis and resonance Raman spectra are very similar to those of ferric myoglobin (Antonini & Brunori, 1971; Egawa et al., 1993), where the heme is ligated axially by a histidine and an H_2O as determined crystallographically (Takano, 1977). The UV–vis band at 632 nm is characteristic of this high-spin species. The frequencies of Raman bands also reveal the presence of a six-coordinate high-spin (6c-HS) heme at pH 6.0 (Table 2). Increasing pH shifts the Soret maximum to the red, accompanied by the gradual disappearance of the 632-nm peak in the UV–vis spectra. In the resonance Raman spectra, the intensities of the bands at 1483 (ν_3) and 1565 cm^{-1} (ν_2) of the 6c-HS ferric heme decrease, while the bands at 1503 (ν_3), 1582 (ν_2), and 1638 cm^{-1} (ν_{10}) grow in intensity. These latter bands are characteristic of six-coordinated low-spin (6c-LS) ferric heme (Evangelista-Kirkup et al., 1985). This can be explained by the ionization of the coordinating H_2O molecule to a hydroxide at alkaline pH. A reversal of Raman intensities

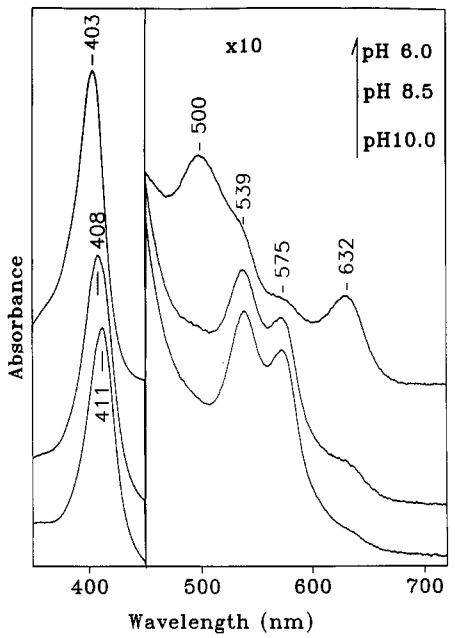

FIGURE 5: UV–vis spectra of Fe(III)PP–HO-1C⁻ at different pHs (~250 μM in capillary tubes).

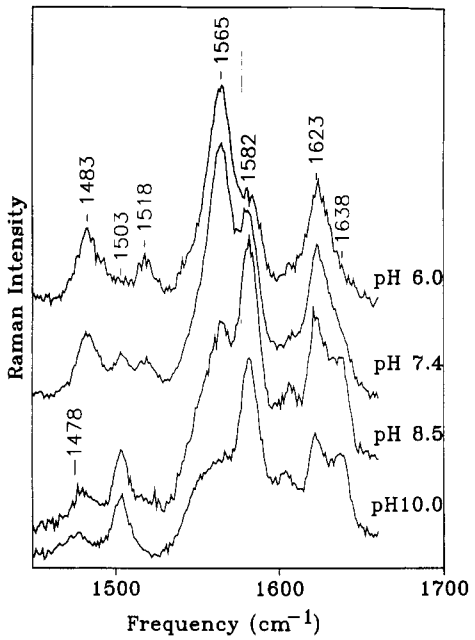

FIGURE 6: Resonance Raman spectra of Fe(III)PP–HO-1C⁻ in the spin- and coordination-state frequency region as a function of pH (413.1-nm excitation).

characteristic of high- and low-spin hemes occurs between pH 7.4 and 8.5 (Figure 6). Even at pH 10.0, high-spin Raman bands still have some intensity. This is expected since hydroxide adducts of hemes generally show thermal equilibrium between high- and low-spin states (Iizuka & Yonetani, 1970). The resonance Raman spectrum of ferric HO-1C⁻ (pH 7.4) obtained at ~90 K (Figure 7) does show an increase in the low-spin population at the expense of the high-spin population. The relative intensity of 1582- (6c-LS) vs 1565-cm⁻¹ (6c-HS) bands increases at lower temperature. Likewise, the relative intensity of 1503 (6c-LS) vs 1483 cm⁻¹ (6c-HS) also increases at ~90 K, although the 1503-cm⁻¹ band has a higher frequency (1511 cm⁻¹) at the low temperature. The important conclusion is that the ferric heme–HO-1C⁻ complex is six-coordinate, with axial ligands donated by a histidine

Table 2: Porphyrin Skeletal Mode Frequencies (cm⁻¹) of Ferric *b* Hemes as a Function of pH

	low/neutral pH (6c-HS)				alkaline pH (6c-LS)[a]				
proteins	ν_2	ν_3	ν_4	ν_{10}	ν_2	ν_3	ν_4	ν_{10}	ref.
heme-HO	1565	1483	1372	1610[b]	1582	1503	1376	1638	this work
Mb	1564	1483	1371		1586	nd[c]	1374	1636	*d,e*
HRP[f]					1581	1508	1379	1635	*g*
CCP[h]	1563	1478	1370	1616	1578	1508	1374	1639	*i*

[a] At alkaline pH, these proteins exhibit a small amount (≈10%) of a 6c-HS hydroxo species in addition to the dominant 6c-LS hydroxo species (see cited references). [b] Determined from resonance Raman spectra obtained with 441.6-nm (pH 6.0) and 514.5-nm excitation (pH 7.4). [c] Not determined. [d] Asher and Schuster (1979). [e] Egawa et al. (1993). [f] The species appear to be 5c-HS under these conditions; there is no evidence for 6c-HS HRP. [g] Palaniappan and Terner (1989). [h] Coexists with 5c-HS species. [i] Smulevich et al. (1988).

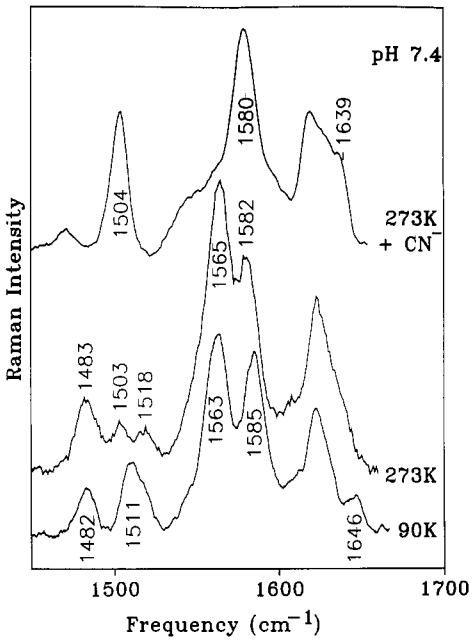

FIGURE 7: Resonance Raman spectra of (i) the cyanide adduct (200-fold excess KCN, pH 7.4) of Fe(III)PP–HO-1C⁻ (upper trace) and (ii) Fe(III)PP–HO-1C⁻ (pH 7.4) at two different temperatures (lower two traces) in the spin- and coordination-state frequency region. The CN⁻ and 90 K traces have been subjected to a 13-point smoothing.

and an H_2O (or OH^- at alkaline pH). The pK_a of this coordinating H_2O can be estimated to be ~8.0 from the relative UV–vis absorbance (Figure 5) and relative Raman intensity of the high- and low-spin hemes. It is interesting to note that ferric horseradish peroxidase (HRP) is five-coordinate and ferric cytochrome *c* peroxidase (CCP) is a mixture of five- and six-coordinate species at low to physiological pH (Table 2) (Rakshit & Spiro, 1974; Choi & Spiro, 1983; Dasgupta et al., 1989; Palaniappan & Terner, 1989; Mylrajan et al., 1990). This behavior is different from ferric heme–heme oxygenase complex which, like myoglobin, exists only as a six-coordinate species.

Further evidence for the coordination of a replaceable water molecule is from a study of the CN⁻ adduct of heme–HO-1C⁻ complex. As shown in Figure 7, the resonance Raman bands for high-spin heme are converted into low-spin heme signals when KCN is added. The observed frequencies of porphyrin skeletal modes (1580, 1504, and 1639 cm⁻¹ for ν_2, ν_3, and ν_{10}, respectively) are characteristic of a 6c-LS heme. Although there are no discernible high-spin signals remaining in the

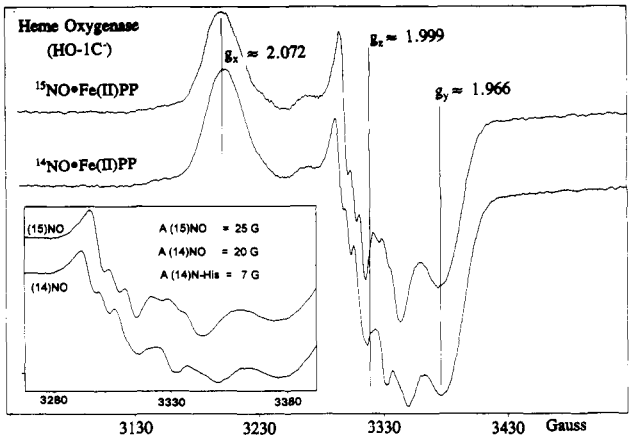

FIGURE 8: X-band EPR spectra of the ^{15}NO (upper trace) and ^{14}NO (lower trace) adducts of Fe(II)PP–HO-1C⁻ at ~5 K and a microwave power of 10 μW. The inset shows an enlargement of the central resonances indicating the hyperfine splittings evident from the use of the two isotopes and the superhyperfine splitting (especially near 3300 G) from the histidine ligand of the heme moiety in heme oxygenase.

presence of 200-fold excess KCN, lower concentrations of KCN (<10-fold) do not produce complete conversion to the low-spin form (data not shown).

Mn(III)PP–Heme Oxygenase Complex. The resonance Raman spectra of Mn(III)PP–HO-1C⁻ complex (data not shown) can almost be superimposed upon those of Mn(III)-PP–Mb and Mn(III)PP–Hb (Parthasarathi & Spiro, 1987). With 476.5-nm excitation, the Raman spectrum of Mn(III)-PP–HO-1C⁻ is dominated by polarized bands at 1373 (ν_4), 1499(ν_3), and 1574(ν_2) cm^{-1}. The lattermost band has a large contribution from the inversely polarized ν_{19} at 1579 cm^{-1}, which makes the local spectral region appear to be depolarized. However, the contribution of ν_{19} is obvious because the peak maxima are different in the parallel and perpendicularly polarized spectra. Moreover, the 1579-cm^{-1} band is clearly observed with 579.3-nm irradiation, as expected for Q-band excitation. The situation for the band at ~1630 cm^{-1} is rather similar. This vinyl mode should be polarized. It has a contribution from the depolarized ν_{10} at 1632 cm^{-1} (which is observed in the perpendicularly polarized spectra excited at 476.5 nm) and with 579.3-nm excitation. The 1555-cm^{-1} band in the 579.3-nm spectrum can be assigned as ν_{11}. The frequencies of all these porphyrin skeletal modes are within 2 cm^{-1} of those observed for Mn(III)PP–Mb or Mn(III)-PP–Hb (Parthasarathi & Spiro, 1987). It has been suggested that those two latter species both have an axial water ligand in aqueous solution, although the crystal structure of Mn-(III)PP–Hb shows that water molecules are within the bonding distance only in α-chains but not in β-chains (Moffat et al., 1976). It is most likely that the axial ligands in the Mn-(III)PP–heme oxygenase complex are a histidine residue and an H_2O molecule, as proposed above for the heme–heme oxygenase complex.

EPR Spectroscopy. The EPR spectrum of the oxidized heme–heme oxygenase HO-1C⁻ complex at ~4 K gives a strongly axial signal with $g_\parallel \approx 6$ and $g_\perp \approx 2$ similar to that of hemin (Blumberg & Peisach, 1973), aquometmyoglobin, lignin peroxidase (Andersson et al., 1985), and manganese peroxidase (Mino et al., 1988) (data not shown). We have also observed the EPR spectra of the NO adducts of the reduced heme–heme oxygenase complex prepared from $Na^{14}NO_2$ and $Na^{15}NO_2$ (Figure 8). These spectra have a rhombic pattern with the principal g values at $g_x \approx 2.07$, $g_y \approx 1.97$, and $g_z \approx 2.00$. The central $g_z \approx 2.00$ absorption shows

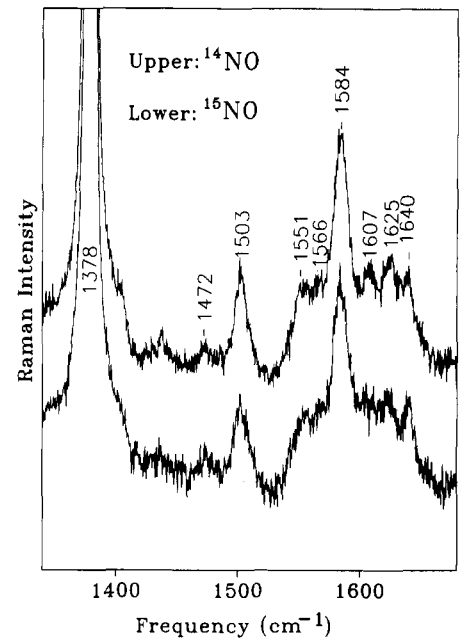

FIGURE 9: Resonance Raman spectra in the high-frequency region of the ^{14}NO (upper trace) and ^{15}NO (lower trace) adducts of Fe-(II)PP–HO-1C⁻ (413.1-nm excitation, ~90 K).

hyperfine interactions from the NO ligand estimated for ^{15}N to be ≈25 G and for ^{14}N to be ≈20 G. In addition, a well-developed superhyperfine structure is evident in the lowest field resonance centered at ~3300 G arising from a second nitrogenous (^{14}N) ligand presumed to be the histidine ligand of the heme moiety (Figure 8, inset). The estimated superhyperfine coupling is 6.5–7 G. The present results are very similar to those reported for HRP and CCP (Yonetani & Yamamoto, 1973; Yonetani et al., 1972) and those of manganese peroxidase (Mino et al., 1988) and strongly support the view that the heme in heme oxygenase is ligated through a histidine axial ligand. The hyperfine splittings of the higher-field resonances are not as well developed in this systems as seen, for example, in HRP (Yonetani et al., 1972) and may be attributable to differential relaxation effects in the frozen solution matrix.

NO Adducts of the Ferrous Heme–Heme Oxygenase Complex. The resonance Raman spectra of the ^{14}NO and ^{15}NO adducts are shown in Figures 9 and 10. The high-frequency porphyrin skeletal modes verify that the heme moieties are six-coordinate and, in general, are comparable with those of the six-coordinate nitrosylmyoglobin (Walters & Spiro, 1982; Mackin et al., 1983). ν_3 at 1503 cm^{-1}, strongly indicative of a six-coordinate species, is nearly identical to that of NOMb, whereas ν_{10} at 1640 is 4 cm^{-1} higher than that in NOMb, but this difference is most probably from the low temperature used in the heme oxygenase measurement. The value of ν_4 at 1378 cm^{-1} is reminiscent of an oxidized heme and suggests electron delocalization in the nitrosyl adduct (ν_4 of the ferrous heme was observed at 1354 cm^{-1}; Figure 2).

Two isotope-sensitive bands are observed in the low-frequency region (Figure 10). The Fe–NO stretching mode can be identified as the band at 566 cm^{-1} (556 cm^{-1} for the ^{15}NO adduct). In NOMb, this frequency was observed at 554 cm^{-1}, which shifts by ~11 cm^{-1} upon ^{15}NO substitution (Hu & Kincaid, 1991; Walters & Spiro, 1982; Tsubaki & Yu, 1982). The higher ν(Fe–NO) observed for heme oxygenase can most easily be explained by a relatively weak iron–histidine bond, the strengths of binding of the ligands on the opposite sides of the heme plane being balanced by the *trans*

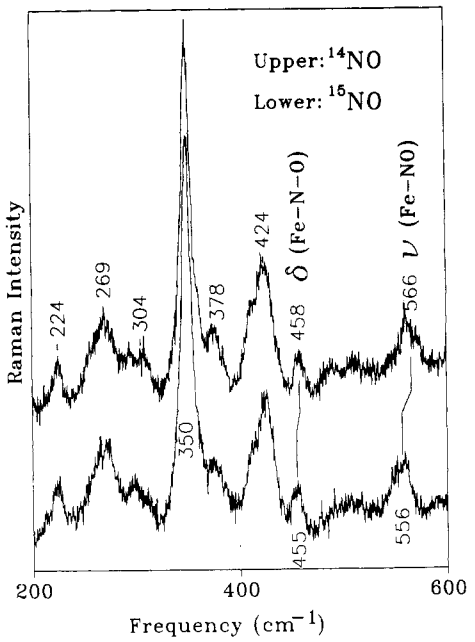

FIGURE 10: Resonance Raman spectra in the low-frequency region of the ^{14}NO (upper trace) and ^{15}NO (lower trace) adducts of Fe(II)PP–HO-1C$^-$ (413.1-nm excitation, ~90 K).

effect. A weak proximal histidine ligation is also indicated by the low Fe–His stretching frequency of 216 cm^{-1} in the ferrous heme–heme oxygenase complex (Figure 3), a value that is ~5 cm^{-1} lower than in ferrous myoglobin. A comparably higher Fe–N–O bending mode may be assigned at 458 cm^{-1} (455 cm^{-1} with ^{15}NO; Figure 10). The δ(Fe–N–O) mode was identified at 449 cm^{-1} for nitrosylmyoglobin by use of NO, ^{15}NO, $N^{18}O$, and $^{15}N^{18}O$ isotopes (Hu & Kincaid, 1991). If the axial ligation strengths of NO and the physiological O_2 are comparable, then the finding that the proximal histidine ligation in the heme–heme oxygenase complex is weak makes the strong implication that, upon binding of O_2, the proximal His bonding is not likely to be significantly increased. Therefore, the electron-donating ability of the proximal histidine, and its role in the oxygen activation process, is limited and must be governed by other interactions in the heme pocket.

Structural and Mechanistic Implications. This study has shown that heme oxygenase binds Fe(III)PP through a histidine residue, with a water molecule (or OH^-) as the other axial ligand. On reduction, the heme remains bound to the histidine residue, and this species is now capable of binding O_2 as a sixth ligand (Wilks & Ortiz de Montellano, 1993a). It is striking that the structure of the heme–heme oxygenase complex resembles that of myoglobin more than those of oxygen-activating heme enzymes. For cytochromes P-450, it is proposed that the proximal cysteine thiolate ligand destabilizes the dioxygen bond through strong electron donation ("push") and a concomitant electron "pull" from a hydrogen-bonding network on the distal side (Gerber & Sligar, 1992). In peroxidases, a similar push/pull mechanism is operative. The proximal histidine, which is either ionized or strongly hydrogen-bonded, plays a similar role as the thiolate ligand of cytochrome P-450. However, its push effect is also not strong enough to promote efficient, heterolytic cleavage of the O–O bond. The presence on the distal side of a histidine and a positively charged arginine further facilitate dioxygen bond cleavage by a pull mechanism (Poulos et al., 1980; Finzel et al., 1984). The fact that the axially coordinated histidine in heme oxygenase appears to be neither ionized nor strongly hydrogen bonded suggests that the distal side of the heme pocket would have to assist dioxygen bond cleavage to a greater extent than it does in the peroxidases if the initial step of the reaction is O–O bond cleavage to give a ferryl species. Recent work suggests, however, that the first step in the reaction sequence catalyzed by heme oxygenase may not be dioxygen bond cleavage (Wilks & Ortiz de Montellano, 1993a,b). Formation of a ferryl species by reaction with alkyl and acyl peroxides has been found to yield a compound II-like ferryl species, but the ferryl species does not lead to biliverdin formation. This suggests that the first step of the heme oxygenase reaction is not heterolytic cleavage of the O–O bond but rather homolytic cleavage or addition of the intact iron-coordinated O_2 molecule to the porphyrin ligand (Wilks & Ortiz de Montellano, 1993). The relative ineffectualness of the imidazole ligand as an electron donor, by making dioxygen bond cleavage less efficient, may actually help to channel the reaction course to biliverdin formation rather than ferryl complex formation.

ACKNOWLEDGMENT

We thank Dr. Simon de Vries (Delft Technical University) for valuable assistance with the EPR experiments and Prof. John Golbeck (University of Nebraska, Lincoln) for the use of his Macintosh EPR data collection program. We are grateful to Dr. Denis L. Rousseau (AT&T Bell Laboratories) for providing us with a preprint of their study on the heme–heme oxygenase complex (Takahashi et al., 1994). This entirely independent work was completed shortly before our present study, and the agreement between similar experiments is excellent. The results of both groups of researchers were presented simultaneously at the 6th International Conference of Bioinorganic Chemistry, San Diego, CA, Aug 23–27, 1993.

REFERENCES

Andersson, L. A., Renganathan, V., Chiu, A. A., Loehr, T. M., & Gold, M. H. (1985) *J. Biol. Chem. 260*, 6080–6087.

Antonini, E., & Brunori, M. (1971) *Hemoglobin and Myoglobin in Their Reactions with Ligands*, pp 17–19, North Holland, Amsterdam.

Asher, S. A., & Schuster, T. M. (1979) *Biochemistry 18*, 5377–5387.

Beale, S. I. (1993) *Chem. Rev. 93*, 785–802.

Blumberg, W. E., & Peisach, J. (1973) in *Oxidases and Related Redox Systems* (King, T. E., Mason, H. S., & Morrison, M., Eds.) pp 299–307, University Park Press, Baltimore, MD.

Bonkovsky, H. L., Healey J. F., & Pohl, J. (1990) *Eur. J. Biochem. 189*, 155–166.

Choi, S., & Spiro, T. G. (1983) *J. Am. Chem. Soc. 105*, 3683–3692.

Choi, S., Spiro, T. G., Langry, K. C., Smith, K. M., Budd, D. L., & La Mar, G. N. (1982) *J. Am. Chem. Soc. 104*, 4345–4351.

Dasgupta, S., Rousseau, D. L., Auni, H., & Yonetani, T. (1989) *J. Biol. Chem. 264*, 654–662.

Egawa, T., Kitagawa, T., & Makino, R. (1993) *Biochemistry 32*, 241–252.

Evangelista-Kirkup, R., Crisanti, M., Poulos, T. L., & Spiro, T. G. (1985) *FEBS Lett. 190*, 221–226.

Evans, C.-O., Healey, J. F., Greene, Y., & Bonkovsky, H. L. (1991) *Biochem. J. 273*, 659–666.

Finzel, B. C., Poulos, T. L., & Kraut, J. (1984) *J. Biol. Chem. 259*, 13027–13036.

Gerber, N. C., & Sligar, S. G. (1992) *J. Am. Chem. Soc. 114*, 8742–8743.

Hu, S., & Kincaid, J. R. (1991) *J. Am. Chem. Soc. 113*, 9760–9766.
Iizuka, T., & Yonetani, T. (1970) *Adv. Biophys. 1*, 157–178.
Ishikawa, K., Sato, M., Ito, M., & Yoshida, T. (1992) *Biochem. Biophys. Res. Commun. 182*, 981–986.
Kincaid, J., Stein, P., & Spiro, T. G. (1979) *Proc. Natl. Acad. Sci. U.S.A. 76*, 549–552; 4156 (errata).
Kitagawa, T., Nagai, K., & Tsubaki, M. (1979) *FEBS Lett. 104*, 376–378.
Kon, H. (1968) *J. Biol. Chem. 243*, 4350–4357.
Kon, H. (1969) *Biochemistry 8*, 4757–4762.
Loehr, T. M., & Sanders-Loehr, J. (1993) *Methods Enzymol. 226*, 431–470.
Loehr, T. M., Keyes, W. E., & Pincus, P. A. (1979) *Anal. Biochem. 96*, 456–463.
Mackin, H. C., Benko, B., Yu, N.-T., & Gersonde, K. (1983) *FEBS Lett. 158*, 199–202.
Maines, M. D. (1988) *FASEB J. 2*, 2557–2568.
Maines, M. D. (1992) *Heme Oxygenase—Clinical Applications and Functions*, CRC Press, Boca Raton, FL.
Maines, M. D., Trakshel, G. M., & Kutty, R. K. (1986) *J. Biol. Chem. 261*, 411–419.
McCoubrey, W. K., Jr., & Maines, M. D. (1993) *Arch. Biochem. Biophys. 302*, 402–408.
Mino, Y., Wariishi, H., Blackburn, N., Loehr, T. M., & Gold, M. H. (1988) *J. Biol. Chem. 263*, 7029–7036.
Moffat, K., Loe, R. S., & Hoffman, B. M. (1976) *J. Mol. Biol. 104*, 669–685.
Mylrajan, M., Valli, K., Wariishi, H., Gold, M. H., & Loehr, T. M. (1990) *Biochemistry 29*, 9617–9623.
Palaniappan, V., & Terner, J. (1989) *J. Biol. Chem. 264*, 16046–16053.
Parthasarathi, N., & Spiro, T. G. (1987) *Inorg. Chem. 26*, 3792–3796.
Poulos, T. L., Freer, S. T., Alden, R. A., Edwards, S. L., Skogland, U., Takio, K., Eriksson, B., Xuong, Ng, H., Yonetani, T., & Kraut, J. (1980) *J. Biol. Chem. 255*, 575–580.
Rakshit, G., & Spiro, T. G. (1974) *Biochemistry 13*, 5317–5323.
Shibahara, S., Muller, R., Taguchi, H., & Yoshida, T. (1985) *Proc. Natl. Acad. Sci. U.S.A. 82*, 7865–7869.
Smulevich, G., Mauro, J. M., Fishel, L. A., English, A. M., Kraut, J., & Spiro, T. G. (1988) *Biochemistry 27*, 5477–5485.
Spiro, T. G., Ed. (1988) *Biological Applications of Raman Spectroscopy*, Vol. III, Wiley, New York.
Spiro, T. G., & Strekas, T. C. (1974) *J. Am. Chem. Soc. 96*, 338–345.
Stevens, C. F., & Wang, Y. (1993) *Nature 364*, 147–148.
Takahashi, S., Wang, J., Rousseau, D. L., Ishikawa, K., Yoshida, T., Host, J. R., & Ikeda-Saito, M. (1994) *J. Biol. Chem.* (in press).
Takano, T. (1977) *J. Mol. Biol. 110*, 537–569.
Tenhunen, R., Marver, H. S., & Schmid, R. (1969) *J. Biol. Chem. 244*, 6388–6394.
Teraoka, J., & Kitagawa, T. (1981) *J. Biol. Chem. 256*, 3969–3977.
Tsubaki, M., & Yu, N.-T. (1982) *Biochemistry 21*, 1140–1144.
Verma, A., Hirsch, D. J., Glatt, C. E., Ronnett, G. V., & Snyder, S. H. (1993) *Science 259*, 381–384.
Walters, M. A., & Spiro, T. G. (1982) *Biochemistry 21*, 6989–6995.
Wilks, A., & Ortiz de Montellano, P. R. (1993a) *J. Biol. Chem. 268*, 22357–22362.
Wilks, A., & Ortiz de Montellano, P. R. (1993b) *J. Inorg. Biochem. 51*, 269.
Yonetani, T., Yamamoto, H., Erman, J. E., Leigh, J. S., Jr., & Reed, G. H. (1972) *J. Biol. Chem. 247*, 2447–2455.
Yoshida, T., & Kikuchi, G. (1978) *J. Biol. Chem. 253*, 4224–4229.
Yoshida, T., & Kikuchi, G. (1979) *J. Biol. Chem. 254*, 4487–4491.
Yoshida, T., Biro, P., Cohen, T., Muller, R., & Shibahara, S. (1988) *Eur. J. Biochem. 171*, 457–461.
Yoshinaga, T., Sassa, S., & Kappas, A. (1982) *J. Biol. Chem. 257*, 7778–7785.
Zhuo, M., Small, S. A., Kandel, E. R., & Hawkins, R. D. (1993) *Science 260*, 1946–1950.